Author/s:
Goodall, KJ;Nguyen, A;McKenzie, C;Eckle, SBG;Sullivan, LC;Andrews, DM

Title:
The murine CD94/NKG2 ligand, Qa-1b, is a high-affinity, functional ligand for the CD8αα homodimer

Date:
2020-03-06

Citation:
Goodall, K. J., Nguyen, A., McKenzie, C., Eckle, S. B. G., Sullivan, L. C. & Andrews, D. M. (2020). The murine CD94/NKG2 ligand, Qa-1b, is a high-affinity, functional ligand for the CD8αα homodimer. Journal of Biological Chemistry, 295 (10), pp.3239-3246. https://doi.org/10.1074/jbc.RA119.010509.

Persistent Link:
https://hdl.handle.net/11343/331893

The murine CD94/NKG2 ligand, Qa-1^b, is a high-affinity, functional ligand for the CD8$\alpha\alpha$ homodimer

Received for publication, August 5, 2019, and in revised form, January 22, 2020 Published, Papers in Press, January 28, 2020, DOI 10.1074/jbc.RA119.010509

Katharine Jennifer Goodall[‡1], Angela Nguyen[‡], Craig McKenzie[‡], Sidonia Barbara Guiomar Eckle[§], Lucy Catherine Sullivan[§2], and Daniel Mark Andrews[‡2,3]

From the [‡]Department of Immunology and Pathology, Central Clinical School, Monash University, Melbourne, Victoria, 3004, Australia and [§]Department of Microbiology and Immunology, Peter Doherty Institute for Infection and Immunity, University of Melbourne, Melbourne, Victoria, 3000, Australia

Edited by Peter Cresswell

The immune co-receptor CD8 molecule (CD8) has two subunits, CD8α and CD8β, which can assemble into homo or heterodimers. Nonclassical (class-Ib) major histocompatibility complex (MHC) molecules (MHC-Ibs) have recently been identified as ligands for the CD8$\alpha\alpha$ homodimer. This was demonstrated by the observation that histocompatibility 2, Q region locus 10 (H2-Q10) is a high-affinity ligand for CD8$\alpha\alpha$ which also binds the MHC-Ib molecule H2-TL. This suggests that MHC-Ib proteins may be an extended source of CD8$\alpha\alpha$ ligands. Expression of H2-T3/TL and H2-Q10 is restricted to the small intestine and liver, respectively, yet CD8$\alpha\alpha$-containing lymphocytes are present more broadly. Therefore, here we sought to determine whether murine CD8$\alpha\alpha$ binds only to tissue-specific MHC-Ib molecules or also to ubiquitously expressed MHC-Ib molecules. Using recombinant proteins and surface plasmon resonance–based binding assays, we show that the MHC-Ib family furnishes multiple binding partners for murine CD8$\alpha\alpha$, including H2-T22 and the CD94/NKG2-A/B-activating NK receptor (NKG2) ligand Qa-1^b. We also demonstrate a hierarchy among MHC-Ib proteins with respect to CD8$\alpha\alpha$ binding, in which Qa-1^b > H2-Q10 > TL. Finally, we provide evidence that Qa-1^b is a functional ligand for CD8$\alpha\alpha$, distinguishing it from its human homologue MHC class I antigen E (HLA-E). These findings provide additional clues as to how CD8$\alpha\alpha$-expressing cells are controlled in different tissues. They also highlight an unexpected immunological divergence of Qa-1^b/HLA-E function, indicating the need for more robust studies of murine MHC-Ib proteins as models for human disease.

There are two distinct subunits of CD8, termed CD8α and CD8β. These can assemble into CD8$\alpha\alpha$ homodimers or CD8$\alpha\beta$ heterodimers (1, 2). The CD8$\alpha\beta$ heterodimer interacts with class I MHC[4] molecules, providing co-stimulation. In contrast, the precise function of the CD8$\alpha\alpha$ homodimer is unknown, but it is thought to act as a co-repressor (3). Although T cells expressing CD8$\alpha\beta$ are primarily TCR$\alpha\beta^+$ and account for the vast majority of peripheral CD8 T cells (2, 4), CD8$\alpha\alpha$ homodimers are the principal recognition element for a large proportion of intestinal epithelial lymphocytes, peripheral TCR$\gamma\delta$ T cells and activated TCR$\gamma\delta$ CD8 T cells (5–10). The only known ligands for CD8$\alpha\alpha$ are H2-T3/TL (11) and H2-Q10 (12) and these belong to the nonclassical class I or MHC-Ib family.

MHC-Ib are less polymorphic than class Ia and can demonstrate cellular and tissue specificity (13, 14). This allows them to serve more diverse and specialized functions than their class Ia counterparts, whose primary role is the presentation of intracellular peptides to CD8 T cells. For example, H2-T3/TL is restricted to epithelial cells of the intestine (15, 16), H2-Q10 is a soluble MHC (17, 18) that is overexpressed in the liver (19), and H2-T13 is only expressed in the blastocyst and placenta (20). In contrast, H2-M3 is widely expressed (13) but is restricted to the presentation of *N*-formylated peptides, making it a recognition element for CD8 T cells directed at intracellular bacteria (21). Similarly, Qa-1^b is ubiquitously expressed (13) and acts to present the leader sequence from class Ia MHC to subsets of natural killer (NK) and T cells expressing CD94/NKG2 heterodimers (22). In this regard, Qa-1^b appears to be the sole homologue of a human MHC-Ib, HLA-E, with which it shares its function (22, 23). As such, studies using Qa-1^b have been heavily utilized as preclinical models for HLA-E responses to a variety of infections and cancers (24, 25).

The observation that H2-T3/TL and H2-Q10 demonstrate tissue-restricted expression whereas CD8$\alpha\alpha$ expressing cells are distributed throughout nonlymphoid organs suggested that other MHC-Ib could act as ligands for CD8$\alpha\alpha$. Our results support this hypothesis and demonstrate that the interaction between MHC-Ib and CD8$\alpha\alpha$ occurs within a hierarchical framework. Surface plasmon resonance demonstrated that Qa-1^b had the highest affinity for CD8$\alpha\alpha$ and was also capable of activating CD8$\alpha\alpha$ expressing T cells. These interactions indicate that CD8$\alpha\alpha$ ligands are more widespread than previously anticipated. Importantly, they also demonstrate a func-

This work was supported by National Health and Medical Research Council (NHMRC) Grant APP1141950 (to L. C. S.). The authors declare that they have no conflicts of interest with the contents of this article.

[1] To whom correspondence should be addressed: Australian Centre for Blood Diseases, Monash University, Melbourne, Victoria, 3004, Australia. Tel.: 61-3-9903-0196; E-mail: katharine.goodall@monash.edu.

[2] These authors contributed equally to this work.

[3] Present address: Bioproperties Pty Ltd, RMIT University Bundoora Campus, Bundoora Victoria, 3083, Australia.

[4] The abbreviations used are: MHC, major histocompatibility complex; MHC-Ib, nonclassical (class-Ib) molecules; NK, natural killer; SPR, surface plasmon resonance; MFI, median fluorescent intensity; CMV, cytomegalovirus; MCMV, murine CMV; HCMV, human CMV; MSCV, murine stem cell virus; RU, response units.

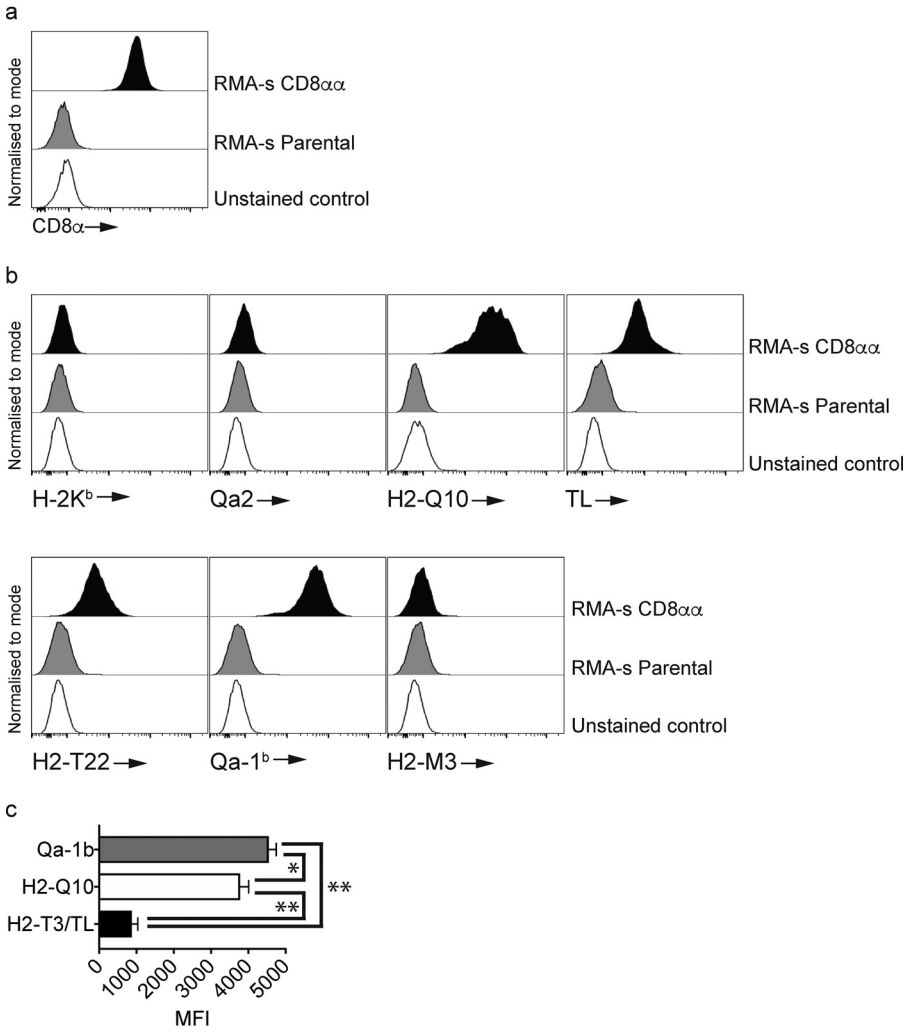

Figure 1. MHC-Ib are an extended family of ligands for CD8αα. Staining of RMA-s–CD8 αα cells with class Ia and MHC-Ib tetramers demonstrates selectivity of class I MHC binding. *a*, staining of CD8α on RMA-s–CD8αα cells. The *open* histogram is the unstained control whereas the *light-shaded* histogram is CD8 staining on RMA-s parental cells. The filled histogram is CD8 staining on RMA-s–CD8αα cells. Results are representative of at least three independent experiments. All histograms have been offset to stack vertically above one another and scaled to maximum count for clarity. *b*, staining of RMA-s–CD8αα cells with class Ia and MHC-Ib tetramers demonstrates that H2-T22, TL, H2-Q10, and Qa-1^b bind CD8αα. The *open* histograms are unstained controls, the *gray* histograms are the indicated tetramers on RMA-s cells and the *filled* histograms are tetramer staining on RMA-s–CD8αα cells. Results are representative of at least three independent experiments. All histograms have been offset to stack vertically above one another and scaled to maximum count for clarity. *c*, median fluorescent intensity (*MFI*) of H2-T3/TL, H2-Q10 and Qa-1^b staining on RMA-s–CD8αα cells. The MFI was pooled from five independent experiments using equivalent tetramer concentrations and identical laser voltages. *, $p = 0.0476$ and **, $p = 0.0079$.

tional divergence between Qa-1^b and HLA-E and highlight the need for more robust studies of murine MHC-Ib as models for human disease.

Results

MHC-Ib are an extended family of ligands for CD8αα

To determine the potential for MHC-Ib to bind CD8, we first generated RMA-s cells expressing CD8αα (Fig. 1*a*), which were then stained with our panel of MHC-Ib tetramers (Fig. 1*b*). In line with previous data that demonstrated a weak affinity for CD8αα (11), we observed no binding of class Ia H-2K^b tetramers to RMA-s-CD8αα$^+$ cells (Fig. 1*b*). Our results demonstrated a specificity among MHC-Ib for CD8αα with binding observed for H2-Q10, H2-T3/TL, H2-T22, and Qa-1^b, but not Qa-2 or H2-M3 (Fig. 1*b*). Furthermore, analysis of the histograms suggested that H2-Q10 and Qa-1^b bound to RMA-s-CD8αα$^+$ cells better than H2-T3/TL. Comparison of median fluorescent intensity (MFI) staining across multiple experiments demonstrated a significant increase in the MFI between H2-T3/TL and H2-Q10 or Qa-1^b (**, $p = 0.0079$) as well as between H2-Q10 and Qa-1^b (*, $p = 0.0476$) (Fig. 1*c*).

Qa-1^b binds CD8αα with a higher affinity than H2-T3/TL and H2-Q10

We have previously demonstrated that the interaction between H2-Q10 and CD8αα is of a higher affinity (~300 nM) than that between H2-T3/TL and CD8αα (~800 nM) (12). Given these observations, we sought to determine the affinity between Qa-1^b and CD8αα as a means to determine a binding hierarchy among H2-T3/TL, H2-Q10, and Qa-1^b. When using Qa-1^b as the ligand (Fig. 2*a*), the K_D calculated was ~300 nM (averaged over several independent experiments, Fig. 2*c*), whereas using Qa-1^b in the analyte phase (Fig. 2*b*), the K_D calculated was ~200 nM (averaged over several independent

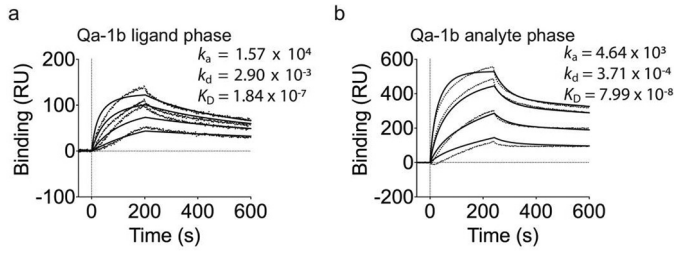

c

	Qa-1b Ligand	Qa-1b Analyte
k_a (x 10^3 $M^{-1}s^{-1}$)	18 ± 5.8	4.7 ± 0.3
k_d (x 10^{-3} s^{-1})	3.4 ± 1.3	0.8 ± 0.2
K_D (x 10^{-7} M)	2.9 ± 1.8	1.9 ± 0.5

Figure 2. Qa-1^b binds CD8αα with high affinity. *a* and *b*, binding of (*a*) decreasing concentrations of CD8αα (1000, 400, 160, and 64 nM; *top to bottom*) to neutravidin-immobilized Qa-1^b or (*b*) decreasing concentrations of Qa-1^b (5000, 2000, 800, and 320 nM; *top to bottom*) to CD8αα captured by an antibody to CD8α (53–6.72), which was immobilized by amine-coupling. Results are presented in response units (*RU*) after subtraction of baseline values. Plots are representative of at least two independent experiments. *Dotted vertical lines* at 0s indicate injection start. *Irregular lines* represent raw data and *solid lines* indicate data fit using a 1:1 Langmuir binding model. *c*, pooled kinetic values from independent SPR experiments, showing mean ± S.E.

experiments, Fig. 2*c*). Therefore, the SPR in the two different orientations yielded broadly consistent results and reinforced our tetramer data. Collectively, the data from Figs. 1 and 2 demonstrate that MHC-Ib represents an extended family of ligands for CD8αα and that a hierarchy exists among these molecules with Qa-1^b currently at the apex.

MHC-Ib binds CD8αα on γδT cells with Qa-1^b inducing IFN-γ production

Having identified Qa-1^b as a high-affinity ligand for CD8αα, we next sought to confirm this interaction directly *ex vivo*. To do this, we isolated lymphocytes from the small intestine of C57BL/6 mice in which a significant proportion of cells are TCRγδ$^+$/CD8αα$^+$ (Fig. 3*a*). Because lymphocytes from the gut also express CD94/NKG2 heterodimers and this can also bind Qa-1^b, we separated intestinal lymphocytes into TCRγδ$^+$/CD8αα$^+$/CD94$^-$ (Fig. 3*a*). In line with our previous data, we observed that TCRγδ$^+$/CD8αα$^+$/CD94$^-$ cells bound TL, H2-Q10, and Qa-1^b in a similar manner to that observed using SPR and our cell line. Sorting of TCRγδ$^+$/CD8αα$^+$/CD94$^-$ cells and culturing them in the presence of crosslinked Qa-1^b resulted in the production of IFN-γ (Fig. 3*b*). This effect was not observed when TCRγδ$^+$/CD8αα$^-$/CD94$^-$ cells were crosslinked (Fig. 3*b*), indicating specificity for CD8αα. These data highlight the capacity of Qa-1^b to act as a functional ligand for TCRγδ$^+$/CD8αα$^+$ lymphocytes.

HLA-E and Qa-1^b differ in their ability to bind to CD8αα

Finally, we sought to determine whether the interaction between Qa-1^b and CD8αα was shared with their human counterparts. To do this, we generated Jurkat cells expressing homodimers of human CD8αα and stained them with tetramers of HLA-E, Qa-1^b, and HLA-G (Fig. 4). In line with a previous study (26), we observed minimal binding of HLA-E and Qa-1^b to human CD8αα. In contrast, we did observe binding of the known human CD8αα ligand HLA-G (Fig. 4*a*). Examination of the reverse interaction indicated that HLA-E and HLA-G had minimal binding to mouse CD8αα (Fig. 4*b*). These data demonstrate that the interaction between Qa-1^b and CD8αα is highly specific and suggest a significant divergence between Qa-1^b and HLA-E with respect to CD8αα binding.

Discussion

Our data provide new evidence that the mouse MHC-Ib provides multiple ligands for CD8αα, expanding on previous observations that identified the prototypical ligand, H2-TL (10, 27, 28) and H2-Q10 (24). The expression pattern of H2-TL is restricted to epithelial cells of the small intestine (15, 16), where it plays a central role in the activation of CD8αα$^+$ cells (29), whereas H2-Q10 is restricted to the liver (19), where it regulates the development of CD8αα$^+$ γδT cells. However, subsets of CD8αα$^+$ cells exist in the lung and kidney (5–10), but none of these organs expresses H2-TL. Our observation that H2-T22 and Qa-1^b are ligands for CD8αα now provides a rationale for the presence of CD8αα expressing cells outside of the small intestine and liver.

The signals controlling the development and activation of CD8αα expressing cells are not completely understood. These cells can be found in mice lacking all class I (30) as well as those lacking just class Ia MHC or H2-TL (29–32). This suggests that the role of MHC-Ib, and in particular Qa-1^b, is more likely to be associated with controlling the responses of CD8αα expressing cells. Interestingly, the immune systems of Qa-1^b–deficient mice develop normally but they do exhibit defects in secondary immune responses (33). The answer to this may lie within the capacity of activated CD8 T cells to up-regulate the CD8αα homodimer (10). Indeed, the expression of CD8αα promotes the survival and differentiation of memory T cell precursors (10). Although an up-regulation of H2-TL is observed on activated antigen-presenting cells (10), our new data suggest that the capacity of H2-TL to bind CD8αα on activated CD8 T cells would be outcompeted by Qa-1^b. Qa-1^b can also be up-regulated on antigen-presenting cells by the actions of TLR ligands and the presence of IFN-γ (34, 35), making it a likely target for activated T cells expressing CD8αα. Intriguingly, activated dendritic cells can stimulate the activation of Qa-1^b restricted TCRγδ cells expressing CD8αα (36). These cells can then target and eliminate self-reactive CD4 T cell clones and attenuate the severity of experimental autoimmune encephalomyelitis (35). Although our experiments did not completely discount the co-expression of additional receptors that might also engage Qa-1^b on CD8αα+ TCRγδ+ cells, our data convincingly showed that Qa-1^b is a *bona fide* ligand for CD8αα itself. Hence, it will be interesting to determine whether CD8αα can act as a co-stimulator or co-repressor of the activation of Qa-1^b restricted CD8αα+ TCRγδ cells. Given that CD8αα does not act as a co-receptor for CD8-dependent TCRs (37, 38) and that H2-TL is thought to act as a co-repressor (3), it is likely that the presence of CD8αα on these Qa-1^b-restricted T cells is limiting their functionality. In addition, it will be important to determine whether binding can occur between Qa-1^b and the CD8αβ heterodimer. It would be expected that if Qa-1^b can interact with CD8αβ, it would be at a significantly lower affinity than to CD8αα, to prevent CD8αβ+ T cells from becoming activated by the presence of Qa-1^b.

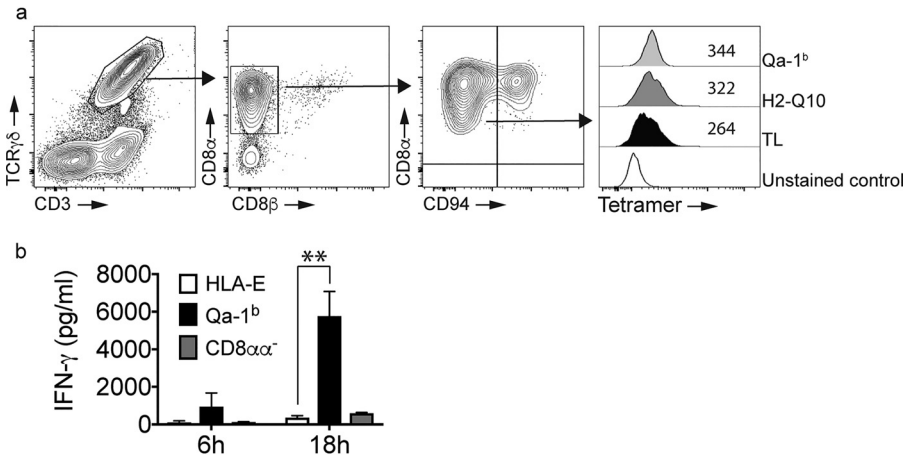

Figure 3. MHC-Ib binds CD8αα on γδT cells with Qa-1^b inducing IFN-γ production. *a*, the pattern of MHC-Ib binding to CD8αα γδT cells is similar to that observed for RMA-s–CD8αα cells. FACS analysis of small intestine identifies a population of CD8αα$^+$/CD94$^-$ γδT cells that bind MHC-Ib tetramers. Contour plots show the staining for CD3$^+$/γδTCR$^+$ cells (*left panel*), their expression of CD8αα and the delineation of CD8αα$^+$/CD94$^-$ and CD8αα$^+$/CD94$^+$ subsets. The *arrows* show the pattern of electronic gating. Staining of TCRγδ$^+$/CD8αα$^+$/CD94$^-$ cells with TL, H2-Q10, and Qa-1^b demonstrates increased binding of Qa-1^b when compared with H2-Q10 and TL. The *open* histogram is unstained, the *filled* histogram is TL, the *dark-shaded* histogram is H2–10 and the *light-shaded* histogram is Qa-1^b. Numbers in the histogram are the median fluorescent intensity. Results are representative of at least four independent experiments. All histograms have been offset to stack vertically above one another and scaled to maximum count for clarity. *b*, Qa-1^b promotes CD8αα γδT cell activation. TCRγδ$^+$/CD8αα$^+$/CD94$^-$ cells were sorted from the small intestine and cultured in the presence of crosslinked HLA-E monomers (*open bars*) or Qa-1^b monomers (*filled bars*). TCRγδ$^+$/CD8αα$^-$/CD94$^-$ cells sorted from the small intestine were cultured in the presence of crosslinked Qa-1b monomers (*gray bars*). At 6 and 18 h post stimulation, the supernatants were harvested and cytokine production assessed using a CBA. The data are pooled from two independent experiments performed in triplicate ($n = 6$). **, $p = 0.0022$.

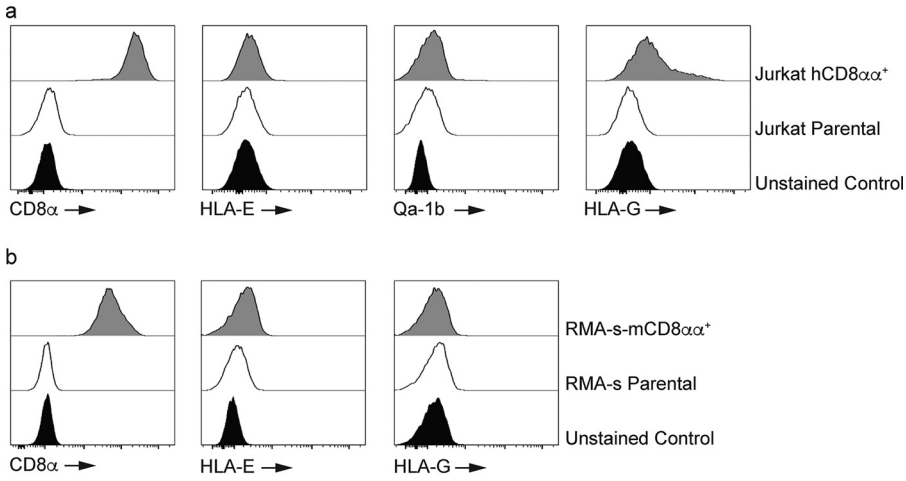

Figure 4. Qa-1b and HLA-E differ in their ability to bind CD8αα. *a*, Jurkat cells were engineered to express human CD8αα (hCD8αα). Antibody staining shows a population of Jurkat-CD8αα cells with high expression of the CD8α homodimer (*left panel*). The *filled* histogram is the unstained control whereas the *open* histogram is CD8 staining on Jurkat cells. The *shaded* histogram is CD8 staining on Jurkat-CD8αα cells. Results are representative of at least two independent experiments. All histograms have been offset to stack vertically above one another and scaled to maximum count for clarity. Tetramer staining shows that HLA-E and Qa-1^b (*second* and *third panels*) have minimal binding to human CD8αα whereas HLA-G (*right panel*) interacts with human CD8αα. The filled histograms are the unstained controls whereas the *open* histograms are tetramer staining on Jurkat cells. The *shaded* histograms are tetramer staining on Jurkat-CD8αα cells. Results are representative of at least two independent experiments. All histograms have been offset to stack vertically above one another and scaled to maximum count for clarity. *b*, HLA-E and HLA-G show minimal interaction with mouse CD8αα (mCD8αα). Antibody staining of RMA-s-mCD8αα cells (*left panel*). The *filled* histogram is the unstained control whereas the *open* histogram is CD8 staining on RMA-s cells. The *shaded* histogram is CD8 staining on RMA-s–mCD8αα cells. Results are representative of at least two independent experiments. All histograms have been offset to stack vertically above one another and scaled to maximum count for clarity. Tetramer staining shows that HLA-E (*middle panel*) and HLA-G (*right panel*) do not bind mouse CD8αα. The *filled* histograms are the unstained controls whereas the open histograms are tetramer staining on RMA-s cells. The *shaded* histograms are tetramer staining on RMA-s–mCD8αα cells. Results are representative of at least three independent experiments. All histograms have been offset to stack vertically above one another and scaled to maximum count for clarity.

Complicating the study of Qa-1^b and CD8αα *in vivo* are the observations that Qa-1^b also binds CD94/NKG2 complexes (22, 39) and the TCR (37). Importantly, HLA-E also binds CD94/NKG2 (23) and the TCR (40) but not CD8αα (Fig. 4). What our data suggest is that Qa-1^b will preferentially bind CD8αα over CD94/NKG2A as the affinity between Qa-1^b and CD8αα is two orders of magnitude higher than that between Qa-1^b and CD94/NKG2A (~17 μM for CD94/NKG2A) (41). The affinity of Qa-1^b-restricted TCRs is yet to be determined but recognition of HLA-E by CMV-specific TCRs ranges from 3 to 37 μM (38, 40). Should these affinities be reflective of those between murine TCRs and Qa-1^b, this suggests that a TCR-independent interaction with CD8αα will predominate. However, further exploration of the responses controlled by Qa-1^b

will require a better understanding of the biochemical partners involved in binding. The observation that CD8αα binds to the α3 region of the MHC (28), whereas CD94/NKG2 and the TCR bind to the α1–2 regions (41, 42) provides a basis for future studies in this area.

The generation of mice in which the Qa-1^b CD8αα interaction is abolished will be an important approach given the observation that Qa-1^b is a high-affinity ligand for CD8αα, whereas HLA-E is not. This is especially relevant given the interest in γδT cells during cytomegalovirus (CMV) infection. Recent evidence has demonstrated that γδT cells confer protection against murine cytomegalovirus infection (MCMV) (43) and the expansion of γδT cell subsets is also associated with the resolution of human cytomegalovirus infection (HCMV) (44). On the flip side, HCMV infection is known to cause a specific expansion of NK cells expressing NKG2C, the ligand for HLA-E (45), whereas this is not seen during MCMV infection (46). Similarly, a large proportion of murine γδT cells express CD8αα (6), although this population is not as pronounced in humans (47, 48). Thus, there is the potential for Qa-1^b to play a major role in the γδT cell response to MCMV, whereas its homologue during HCMV infection involves an NK cell response, mediated by the interaction between HLA-E and NKG2C. Collectively, this indicates that there are alternate strategies for immunity involving analogous molecules in different species. Given the interest in Qa-1^b/HLA-E in models of transplantation (49) and cancer (25) our results provide the basis for the generation of preclinical mouse models that are a more faithful representation of the human condition.

Given that CD8αα recognition occurs within a hierarchy, further investigation into other members of the mouse MHC-Ib is required. We currently understand the basic biochemistry and immunology of only 6 of the 30 MHC-Ib, hence the capacity for future research into the function of this family is warranted. Indeed, it remains possible that many other members of the MHC-Ib family bind CD8αα, and even that another MHC-Ib may eclipse Qa-1^b as the apex partner.

Experimental procedures

Mice

C57BL/6 mice were from Alfred Medical Research and Education Precinct (AMREP) Animal services. All mice were used at between 6 and 8 weeks of age. All experiments were in accordance with the animal ethics guidelines of the National Health and Medical Research Council of Australia and were approved by the AMREP Animal Ethics Committee.

Cell culture

RMA-s and Jurkat cells were sourced from the Peter MacCallum Cancer Centre Tumor cell bank. Cells were cultured in RPMI supplemented with 10% FCS, L-glutamine, penicillin and streptomycin. 293T and Phoenix E cells were cultured in DMEM supplemented with 10% FCS, L-glutamine, penicillin and streptomycin.

Cloning and expression of recombinant CD8

A codon-optimized gene encoding the full-length mouse CD8α (NM_001081110.2) was purchased from GenScript (Piscataway, NJ) and ligated into MSCV vectors. Orientation and correct sequence was confirmed by DNA sequencing using T7 forward and reverse primers.

Retroviral transduction

Retroviral transduction was performed on RMA-s and Jurkat cells; retrovirus-containing supernatant was produced by transfecting packaging cells with murine stem cell virus–internal ribosome entry site–GFP (MSCV-I-GFP) or MSCV-I-mCherry using standard calcium phosphate transfection methods. Viral supernatant was used to transduce RMA-s and Jurkat cells on retronectin (TaKaRa Bio, Shiga, Japan) precoated plates (BD Biosciences). After 5–7 days, GFP only (CD8αα) events were subjected to two rounds of cell sorting (FACSAria, BD Biosciences) to produce stable cell lines. Expression of CD8αα was confirmed by flow cytometry.

Generation of recombinant CD8αα

The sequence of soluble mouse CD8αα, allele CD8A*02, was designed based on a previously published sequence to fold soluble mouse CD8α/CD8β following *Escherichia coli* expression (50), GenBank accession number GQ247790.1, except for the following modifications whereby residue numbering is based on Kern *et al.* (50). (i) Cys-36 was mutated to Ser as based on crystal structures of CD8αα, Cys-36 is not involved in disulfide bonds (50, 51), and we suspected that mutating this residue might improve folding efficiency; (ii) the gene was shorted to cover residues Gly-5 to Lys-128, as in previously determined crystal structures that included mouse CD8αα or CD8αβ there were no data beyond this region; (iii) the gene was codon-optimized for *E. coli* expression by GenScript (Piscataway, NJ). The gene was purchased from GenScript (Piscataway, NJ) and subcloned into a pET30 expression vector, expressed in BL21 *E. coli* competent cells and purified from inclusion bodies. The inclusion bodies were solubilized in 6 M guanidine-HCl and 120 mg/liter of total protein (split over three injections) was rapidly diluted in a buffer containing 0.4 M arginine hydrocholoride, 100 mM Tris-HCl (pH 8), 2 mM EDTA, 3 mM reduced GSH, and 0.3 mM oxidized GSH and allowed to sit for 2–3 days at 4 °C. The refold was then dialyzed against 25 mM HEPES (pH 7.4) overnight, followed by filtration through a 0.45 μM filter. The CD8αα was purified by cation exchange using an SP-Sepharose column (Amersham Biosciences) and eluted using 25 mM HEPES containing a gradient of NaCl. The major peak was pooled, concentrated, and further purified by size exclusion chromatography using Superdex 75 column with a buffer containing 25 mM HEPES (pH 7.4) with 150 mM NaCl.

Generation of tetramers

cDNA encoding residues 20–274 of Qa-2, H2-Q10, H2-TL, and Qa-1^b were generated by GenScript and cloned into a pUC57 vector. H2-M3 and H-2K^b were generated following reverse transcription of cDNA encoding residues 20–274. The cDNA encoding residues 20–274 of H2-T22 were provided by K. Christopher Garcia (Stanford University, CA). All MHC sequences were subcloned into a pET-30–based vector that allowed for an in-frame fusion of a substrate peptide for the

enzyme BirA. The heavy chains of H-2K^b, Qa-2, H2-Q10, TL, H2-T22, Qa-1^b, H2-M3, and mouse β2-microglobulin were expressed separately in *E. coli*, purified from inclusion bodies and refolded in the absence of peptide (H2-TL and H2-T22) or in the presence of OVA (SIINFEKL) for H-2K^b, cofilin (KLTGIKHEL) for Qa-2, ribophorin (VGITNVDL) for H2-Q10, Qdm (AMAPRTLL) for Qa-1^b, and LemA (fMIGWII) for H2-M3. Monomers were purified by anion exchange and size exclusion chromatography, prior to biotinylation with BirA. 100% biotinylation of monomers was confirmed using native gel shift analysis by combining monomer with unlabeled streptavidin (data not shown).

Flow cytometry

Flow cytometric analysis—Small intestines were collected from WT mice and single-cell suspensions prepared using standard protocols. Following resuspension, nonspecific receptors were blocked with mAb 2.4G2, then cells (5×10^6) were stained with mAb to CD8α (53–6.72; BioLegend, San Diego, CA), CD8β (53–5.8; BioLegend), TCR$\gamma\delta$ (GL3; BioLegend), CD3 (17A2; BioLegend), and CD94 (DX22; BioLegend). Cells stained with tetramers were fixed in 2% paraformaldehyde, washed twice in PBS before being resuspended in FACS buffer (PBS–2% FCS). For acquisition, events were electronically gated on FSC-A *versus* FSC-H (singlets), followed by FSC-A and SSC-A (to exclude doublets and debris). Among the remaining population at least 5000 electronic events for CD8$\alpha\alpha$ expressing cells (TCR$\gamma\delta^+$/CD3$^+$/CD8α^+/CD8β^-/CD94$^-$) were collected using an LSR-II or X-20 Fortessa (BD Biosciences). For sorting, events were electronically gated on FSC-A *versus* FSC-H (singlets), followed by FSC-A and SSC-A (to exclude doublets and debris). Among the remaining population CD8$\alpha\alpha^+$ (TCR$\gamma\delta^+$/CD3$^+$/CD8α^+/CD8β^-/CD94$^-$) or CD8$\alpha\alpha^-$ (TCR$\gamma\delta^+$/CD3$^+$/CD8α^-/CD8β^-/CD94$^-$) were sorted to >90% purity.

Activation and analysis of sorted γδT cells—Sorted cells were cultured in RPMI supplemented with 10% FCS, L-glutamine, penicillin, and streptomycin. 10^5 CD8$\alpha\alpha^+$ or CD8$\alpha\alpha^-$ subsets in 100 μl were added to U-bottom 96-well plates in which 5 μg/ml Qa-1^b or HLA-E had been crosslinked overnight at 4 °C. Supernatants were harvested at 6 and 18 h post stimulation and frozen at −20 °C. The CBA Flex System Kit (BD Biosciences) was then used to measure IFN-γ production according to the manufacturer's protocols.

Flow cytometric analysis of RMA-s and Jurkat—Cells were cultured in tissue culture flasks for 2 days prior to removal with Tryple (Invitrogen). Cells were washed two times in PBS and nonspecific binding blocked with 2.4G2. Cells were then stained with mAb to CD8α (mouse 53–6.72, human SK1; BioLegend, San Diego, CA), and tetramers prior to fixation in 2% paraformaldehyde. Cells were then washed twice in PBS, resuspended in FACS buffer and acquired on an LSR-II or X-20 Fortessa flow cytometer (BD Biosciences). Doublets were excluded using a FSC-A *versus* FSC-H acquisition profile followed a FSC-A *versus* SSC-A profile to exclude debris. At least 10,000 gated events were collected for analysis.

Surface plasmon resonance

Surface plasmon resonance (SPR) was performed essentially as described (52) in two different orientations, one where Qa-1^b was on the chip (ligand) and the other where Qa-1^b was in solution (analyte). For Qa-1^b in the ligand phase, biotinylated MHC was captured on the surface of a ProteOn NLC neutravidin chip (Bio-Rad, ~150 RU of each). An empty flow cell with neutravidin alone served as a control. Serially diluted CD8$\alpha\alpha$, produced as described above, was injected simultaneously over the control and test surfaces. To verify results, SPR was also performed in the reverse orientation. In these experiments, an antibody to CD8$\alpha\alpha$ (53–6.72) was amine coupled to two flow cells of a ProteOn GLC chip (~500 RU) and recombinant CD8$\alpha\alpha$ was injected over the chip at 30 μl/min, and ~500 RU was captured by the antibody. The running and sample buffer was 10 mM HEPES (pH 7.4), 150 mM NaCl, and 0.05% Tween-20. The other flow cell containing antibody alone served as a control cell. Qa-1^b was then injected over both flow cells. After subtraction of data from the control flow cells, K_D was calculated by kinetic analysis using the ProteOn Manager software (Bio-Rad). At least two independent SPR experiments were performed in both orientations.

Statistical analysis

The nonparametric, two-tailed Mann-Whitney *U* test was used to determine the statistical significance of data sets; *p* values of less than 0.05 were considered significant.

Author contributions—K. J. G., L. C. S., and D. M. A. conceptualization; K. J. G., A. N., C. M., S. B. G. E., L. C. S., and D. M. A. data curation; K. J. G., L. C. S., and D. M. A. formal analysis; K. J. G., L. C. S., and D. M. A. validation; K. J. G., A. N., C. M., S. B. G. E., L. C. S., and D. M. A. investigation; K. J. G. and D. M. A. visualization; K. J. G., A. N., C. M., S. B. G. E., L. C. S., and D. M. A. methodology; K. J. G. writing-original draft; K. J. G. and D. M. A. project administration; K. J. G., A. N., L. C. S., and D. M. A. writing-review and editing; L. C. S. and D. M. A. funding acquisition; D. M. A. resources; D. M. A. supervision.

Acknowledgments—We thank the members of the Alfred Medical Research and Education Precinct (AMREP) Flow Cytometry unit and the Monash Animal Research Platform.

References

1. DiSanto, J. P., Knowles, R. W., and Flomenberg, N. (1988) The human Lyt-3 molecule requires CD8 for cell surface expression. *EMBO J.* **7,** 3465–3470 CrossRef Medline
2. Norment, A. M., and Littman, D. R. (1988) A second subunit of CD8 is expressed in human T cells. *EMBO J.* **7,** 3433–3439 CrossRef Medline
3. Cheroutre, H., and Lambolez, F. (2008) Doubting the TCR coreceptor function of CD8$\alpha\alpha$. *Immunity* **28,** 149–159 CrossRef Medline
4. Torres-Nagel, N., Kraus, E., Brown, M. H., Tiefenthaler, G., Mitnacht, R., Williams, A. F., and Hünig, T. (1992) Differential thymus dependence of rat CD8 isoform expression. *Eur. J. Immunol.* **22,** 2841–2848 CrossRef Medline
5. Guy-Grand, D., Cerf-Bensussan, N., Malissen, B., Malassis-Seris, M., Briottet, C., and Vassalli, P. (1991) Two gut intraepithelial CD8+ lymphocyte populations with different T cell receptors: A role for the gut epithelium in T cell differentiation. *J. Exp. Med.* **173,** 471–481 CrossRef Medline

6. Sato, K., Ohtsuka, K., Watanabe, H., Asakura, H., and Abo, T. (1993) Detailed characterization of gamma delta T cells within the organs in mice: Classification into three groups. *Immunology* **80,** 380–387 Medline
7. Terry, L. A., DiSanto, J. P., Small, T. N., and Flomenberg, N. (1990) Differential expression and regulation of the human CD8α and CD8β chains. *Tissue Antigens* **35,** 82–91 CrossRef Medline
8. Vremec, D., Zorbas, M., Scollay, R., Saunders, D. J., Ardavin, C. F., Wu, L., and Shortman, K. (1992) The surface phenotype of dendritic cells purified from mouse thymus and spleen: Investigation of the CD8 expression by a subpopulation of dendritic cells. *J. Exp. Med.* **176,** 47–58 CrossRef Medline
9. Ohtsuka, K., Iiai, T., Watanabe, H., Tanaka, T., Miyasaka, M., Sato, K., Asakura, H., and Abo, T. (1994) Similarities and differences between extrathymic T cells residing in mouse liver and intestine. *Cell Immunol.* **153,** 52–66 CrossRef Medline
10. Madakamutil, L. T., Christen, U., Lena, C. J., Wang-Zhu, Y., Attinger, A., Sundarrajan, M., Ellmeier, W., von Herrath, M. G., Jensen, P., Littman, D. R., and Cheroutre, H. (2004) CD8$\alpha\alpha$-mediated survival and differentiation of CD8 memory T cell precursors. *Science* **304,** 590–593 CrossRef Medline
11. Leishman, A. J., Naidenko, O. V., Attinger, A., Koning, F., Lena, C. J., Xiong, Y., Chang, H. C., Reinherz, E., Kronenberg, M., and Cheroutre, H. (2001) T cell responses modulated through interaction between CD8$\alpha\alpha$ and the nonclassical MHC class I molecule, TL. *Science* **294,** 1936–1939 CrossRef Medline
12. Goodall, K. J., Nguyen, A., Matsumoto, A., McMullen, J. R., Eckle, S. B., Bertolino, P., Sullivan, L. C., and Andrews, D. M. (2019) Multiple receptors converge on H2-Q10 to regulate NK and $\gamma\delta$T-cell development. *Immunol. Cell Biol.* **97,** 326–339 CrossRef Medline
13. Ohtsuka, M., Inoko, H., Kulski, J. K., and Yoshimura, S. (2008) Major histocompatibility complex (Mhc) MHC-Ib gene duplications, organization and expression patterns in mouse strain C57BL/6. *BMC Genomics* **9,** 178 CrossRef Medline
14. Wei, X. H., and Orr, H. T. (1990) Differential expression of HLA-E, HLA-F, and HLA-G transcripts in human tissue. *Hum. Immunol.* **29,** 131–142 CrossRef Medline
15. Hershberg, R., Eghtesady, P., Sydora, B., Brorson, K., Cheroutre, H., Modlin, R., and Kronenberg, M. (1990) Expression of the thymus leukemia antigen in mouse intestinal epithelium. *Proc. Natl. Acad. Sci. U.S.A.* **87,** 9727–9731 CrossRef Medline
16. Wu, M., van Kaer, L., Itohara, S., and Tonegawa, S. (1991) Highly restricted expression of the thymus leukemia antigens on intestinal epithelial cells. *J. Exp. Med.* **174,** 213–218 CrossRef Medline
17. Kress, M., Cosman, D., Khoury, G., and Jay, G. (1983) Secretion of a transplantation-related antigen. *Cell* **34,** 189–196 CrossRef Medline
18. Lew, A. M., Maloy, W. L., and Coligan, J. E. (1986) Characteristics of the expression of the murine soluble class I molecule (Q10). *J. Immunol.* **136,** 254–258 Medline
19. Cosman, D., Kress, M., Khoury, G., and Jay, G. (1982) Tissue-specific expression of an unusual H-2 (class I)-related gene. *Proc. Natl. Acad. Sci. U.S.A.* **79,** 4947–4951 CrossRef Medline
20. Sipes, S. L., Medaglia, M. V., Stabley, D. L., DeBruyn, C. S., Alden, M. S., Catenacci, V., and Landel, C. P. (1996) A new major histocompatibility complex class I b gene expressed in the mouse blastocyst and placenta. *Immunogenetics* **45,** 108–120 CrossRef Medline
21. Wang, C. R., Castaño, A. R., Peterson, P. A., Slaughter, C., Lindahl, K. F., and Deisenhofer, J. (1995) Nonclassical binding of formylated peptide in crystal structure of the MHC class Ib molecule H2-M3. *Cell* **82,** 655–664 CrossRef Medline
22. Vance, R. E., Jamieson, A. M., and Raulet, D. H. (1999) Recognition of the class Ib molecule Qa-1(b) by putative activating receptors CD94/NKG2C and CD94/NKG2E on mouse natural killer cells. *J. Exp. Med.* **190,** 1801–1812 CrossRef Medline
23. Braud, V. M., Allan, D. S., O'Callaghan, C. A., Söderström, K., D'Andrea, A., Ogg, G. S., Lazetic, S., Young, N. T., Bell, J. I., Phillips, J. H., Lanier, L. L., and McMichael, A. J. (1998) HLA-E binds to natural killer cell receptors CD94/NKG2A, B and C. *Nature* **391,** 795–799 CrossRef Medline
24. Goodall, K. J., Nguyen, A., Sullivan, L. C., and Andrews, D. M. (2018) The expanding role of murine class Ib MHC in the development and activation of natural killer cells. *Mol. Immunol.* **115,** 31–38 CrossRef Medline
25. Godfrey, D. I., Le Nours, J., Andrews, D. M., Uldrich, A. P., and Rossjohn, J. (2018) Unconventional T cell targets for cancer immunotherapy. *Immunity* **48,** 453–473 CrossRef Medline
26. Gao, G. F., Willcox, B. E., Wyer, J. R., Boulter, J. M., O'Callaghan, C. A., Maenaka, K., Stuart, D. I., Jones, E. Y., Van Der Merwe, P. A., Bell, J. I., and Jakobsen, B. K. (2000) Classical and nonclassical class I major histocompatibility complex molecules exhibit subtle conformational differences that affect binding to CD8$\alpha\alpha$. *J. Biol. Chem.* **275,** 15232–15238 CrossRef Medline
27. Attinger, A., Devine, L., Wang-Zhu, Y., Martin, D., Wang, J. H., Reinherz, E. L., Kronenberg, M., Cheroutre, H., and Kavathas, P. (2005) Molecular basis for the high affinity interaction between the thymic leukemia antigen and the CD8$\alpha\alpha$ molecule. *J. Immunol.* **174,** 3501–3507 CrossRef Medline
28. Liu, Y., Xiong, Y., Naidenko, O. V., Liu, J. H., Zhang, R., Joachimiak, A., Kronenberg, M., Cheroutre, H., Reinherz, E. L., and Wang, J. H. (2003) The crystal structure of a TL/CD8$\alpha\alpha$ complex at 2.1 A resolution: Implications for modulation of T cell activation and memory. *Immunity* **18,** 205–215 CrossRef Medline
29. Olivares-Villagómez, D., Mendez-Fernandez, Y. V., Parekh, V. V., Lalani, S., Vincent, T. L., Cheroutre, H., and Van Kaer, L. (2008) Thymus leukemia antigen controls intraepithelial lymphocyte function and inflammatory bowel disease. *Proc. Natl. Acad. Sci. U.S.A.* **105,** 17931–17936 CrossRef Medline
30. Correa, I., Bix, M., Liao, N. S., Zijlstra, M., Jaenisch, R., and Raulet, D. (1992) Most $\gamma\delta$ T cells develop normally in β 2-microglobulin-deficient mice. *Proc. Natl. Acad. Sci. U.S.A.* **89,** 653–657 CrossRef Medline
31. Gapin, L., Cheroutre, H., and Kronenberg, M. (1999) Cutting edge: TCR alpha beta+ CD8 $\alpha\alpha$+ T cells are found in intestinal intraepithelial lymphocytes of mice that lack classical MHC class I molecules. *J. Immunol.* **163,** 4100–4104 Medline
32. Park, S. H., Guy-Grand, D., Lemonnier, F. A., Wang, C. R., Bendelac, A., and Jabri, B. (1999) Selection and expansion of CD8$\alpha\alpha$(1) T cell receptor α/β(1) intestinal intraepithelial lymphocytes in the absence of both classical major histocompatibility complex class I and nonclassical CD1 molecules. *J. Exp. Med.* **190,** 885–890 CrossRef Medline
33. Hu, D., Ikizawa, K., Lu, L., Sanchirico, M. E., Shinohara, M. L., and Cantor, H. (2004) Analysis of regulatory CD8 T cells in Qa-1-deficient mice. *Nat. Immunol.* **5,** 516–523 CrossRef Medline
34. Colmenero, P., Zhang, A. L., Qian, T., Linrong, L., Cantor, H., Soderstrom, K., and Engleman, E. G. (2007) Qa-1^b-dependent modulation of dendritic cell and NK cell cross-talk in vivo. *J. Immunol.* **179,** 4608–4615 CrossRef Medline
35. Smith, T. R. F., Tang, X., Maricic, I., Garcia, Z., Fanchiang, S., and Kumar, V. (2009) Dendritic cells use endocytic pathway for cross-priming Class Ib MHC-restricted CD8$\alpha\alpha$+TCRab+ T cells with regulatory properties. *J. Immunol.* **182,** 6959–6968 CrossRef Medline
36. Tang, X., Maricic, I., and Kumar, V. (2007) Anti-TCR antibody treatment activates a novel population of nonintestinal CD8$\alpha\alpha$+ TCRab+ regulatory cells and prevents autoimmune encephalomyelitis. *J. Immunol.* **178,** 6043–6050 CrossRef Medline
37. McNicol, A. M., Bendle, G., Holler, A., Matjeka, T., Dalton, E., Rettig, L., Zamoyska, R., Uckert, W., Xue, S. A., and Stauss, H. J. (2007) CD8α/α homodimers fail to function as co-receptor for a CD8-dependent TCR. *Eur. J. Immunol.* **37,** 1634–1641 CrossRef Medline
38. Sullivan, L. C., Walpole, N. G., Farenc, C., Pietra, G., Sum, M. J. W., Clements, C. S., Lee, E. J., Beddoe, T., Falco, M., Mingari, M. C., Moretta, L., Gras, S., Rossjohn, J., and Brooks, A. G. (2017) A conserved energetic footprint underpins recognition of human leukocyte antigen-E by two distinct $\alpha\beta$ T cell receptors. *J. Biol. Chem.* **292,** 21149–21158 CrossRef Medline
39. Doorduijn, E. M., Sluijter, M., Querido, B. J., Seidel, U. J. E., Oliveira, C. C., van der Burg, S. H., and van Hall, T. (2018) T cells engaging the conserved MHC class Ib molecule Qa-1 (b) with TAP-independent peptides are semi-invariant lymphocytes. *Front. Immunol.* **9,** 60 CrossRef Medline
40. Hoare, H. L., Sullivan, L. C., Pietra, G., Clements, C. S., Lee, E. J., Ely, L. K., Beddoe, T., Falco, M., Kjer-Nielsen, L., Reid, H. H., McCluskey, J., Moretta, L., Rossjohn, J., and Brooks, A. G. (2006) Structural basis for a

major histocompatibility complex class Ib-restricted T cell response. *Nat. Immunol.* **7,** 256–264 CrossRef Medline

41. Zeng, L., Sullivan, L. C., Vivian, J. P., Walpole, N. G., Harpur, C. M., Rossjohn, J., Clements, C. S., and Brooks, A. G. (2012) A structural basis for antigen presentation by the MHC class Ib molecule, Qa-1b. *J. Immunol.* **188,** 302–310 CrossRef Medline
42. Kaiser, B. K., Pizarro, J. C., Kerns, J., and Strong, R. K. (2008) Structural basis for NKG2A/CD94 recognition of HLA-E. *Proc. Natl. Acad. Sci. U.S.A.* **105,** 6696–6701 CrossRef Medline
43. Khairallah, C., Netzer, S., Villacreces, A., Juzan, M., Rousseau, B., Dulanto, S., Giese, A., Costet, P., Praloran, V., Moreau, J. F., Dubus, P., Vermijlen, D., Déchanet-Merville, J., and Capone, M. (2015) γδ T cells confer protection against murine cytomegalovirus (MCMV). *PLoS Pathog.* **11,** e1004702 CrossRef Medline
44. Lafarge, X., Merville, P., Cazin, M. C., Bergé, F., Potaux, L., Moreau, J. F., and Déchanet-Merville, J. (2001) Cytomegalovirus infection in transplant recipients resolves when circulating γδ T lymphocytes expand, suggesting a protective antiviral role. *J. Infect. Dis.* **184,** 533–541 CrossRef Medline
45. Lopez-Vergès, S., Milush, J. M., Schwartz, B. S., Pando, M. J., Jarjoura, J., York, V. A., Houchins, J. P., Miller, S., Kang, S. M., Norris, P. J., Nixon, D. F., and Lanier, L. L. (2011) Expansion of a unique CD57(+)NKG2Chi natural killer cell subset during acute human cytomegalovirus infection. *Proc. Natl. Acad. Sci. U.S.A.* **108,** 14725–14732 CrossRef Medline
46. Della Chiesa, M., Sivori, S., Carlomagno, S., Moretta, L., and Moretta, A. (2015) Activating KIRs and NKG2C in viral infections: Toward NK cell memory? *Front. Immunol.* **6,** 573 CrossRef Medline
47. Kadivar, M., Petersson, J., Svensson, L., and Marsal, J. (2016) CD8αβ+ γδ T cells: A novel T cell subset with a potential role in inflammatory bowel disease. *J. Immunol.* **197,** 4584–4592 CrossRef Medline
48. Kenna, T., Golden-Mason, L., Norris, S., Hegarty, J. E., O'Farrelly, C., and Doherty, D. G. (2004) Distinct subpopulations of γδ T cells are present in normal and tumor-bearing human liver. *Clin. Immunol.* **113,** 56–63 CrossRef Medline
49. Sullivan, L. C., Westall, G. P., Widjaja, J. M., Mifsud, N. A., Nguyen, T. H., Meehan, A. C., Kotsimbos, T. C., and Brooks, A. G. (2015) The presence of HLA-E-restricted, CMV-specific CD8+ T cells in the blood of lung transplant recipients correlates with chronic allograft rejection. *PLoS One* **10,** e0135972 CrossRef Medline
50. Kern, P., Hussey, R. E., Spoerl, R., Reinherz, E. L., and Chang, H. C. (1999) Expression, purification, and functional analysis of murine ectodomain fragments of CD8αα and CD8αβ dimers. *J. Biol. Chem.* **274,** 27237–27243 CrossRef Medline
51. Kern, P. S., Teng, M. K., Smolyar, A., Liu, J. H., Liu, J., Hussey, R. E., Spoerl, R., Chang, H. C., Reinherz, E. L., and Wang, J. H. (1998) Structural basis of CD8 coreceptor function revealed by crystallographic analysis of a murine CD8αα ectodomain fragment in complex with H-2Kb. *Immunity* **9,** 519–530 CrossRef Medline
52. Andrews, D. M., Sullivan, L. C., Baschuk, N., Chan, C. J., Berry, R., Cotterell, C. L., Lin, J., Halse, H., Watt, S. V., Poursine-Laurent, J., Wang, C. R., Scalzo, A. A., Yokoyama, W. M., Rossjohn, J., Brooks, A. G., and Smyth, M. J. (2012) Recognition of the nonclassical MHC class I molecule H2-M3 by the receptor Ly49A regulates the licensing and activation of NK cells. *Nat. Immunol.* **13,** 1171–1177 CrossRef Medline